

See discussions, stats, and author profiles for this publication at: <https://www.researchgate.net/publication/338712102>

Conspicuous temperature extremes over Southeast Asia: seasonal variations under 1.5 °C and 2 °C global warming

Article in *Climatic Change* · January 2020

CITATIONS

6

READS

237

7 authors, including:



Shoupeng Zhu

Nanjing University of Information Science & Technology

31 PUBLICATIONS 61 CITATIONS

[SEE PROFILE](#)



Fei Ge

Chengdu University of Information Technology

19 PUBLICATIONS 139 CITATIONS

[SEE PROFILE](#)



Yi Fan

Nanjing University of Information Science & Technology

8 PUBLICATIONS 39 CITATIONS

[SEE PROFILE](#)



Ling Zhang

Nanjing University of Information Science & Technology

25 PUBLICATIONS 308 CITATIONS

[SEE PROFILE](#)

Some of the authors of this publication are also working on these related projects:



Application of Machine Learning in Weather and Climate Prediction [View project](#)



Calibrations of the NWP products [View project](#)



Conspicuous temperature extremes over Southeast Asia: seasonal variations under 1.5 °C and 2 °C global warming

Shoupeng Zhu^{1,3} · Fei Ge^{2,3}  · Yi Fan^{1,4} · Ling Zhang¹ · Frank Sielmann⁵ · Klaus Fraedrich³ · Xiefei Zhi¹

Received: 27 February 2019 / Accepted: 17 December 2019 / Published online: 18 January 2020
© Springer Nature B.V. 2020

Abstract

Guided by the Paris Agreement, the IPCC Special Report on Global Warming of 1.5 °C reported potential risks of climate change at different global warming levels (GWLs). To provide fundamental information on future temperature extremes over Southeast Asia (SEA), projected changes in temperature extreme indices are evaluated for different seasons at 1.5 °C and 2 °C GWLs against the historical reference period of 1976–2005 based on the ensemble of CORDEX simulations. Results show that the temperature indices increase significantly across the Indochina Peninsula and Maritime Continent at both GWLs except for decreasing daily temperature range (DTR) in the dry season, with more pronounced magnitudes at 2 °C GWL. Moreover, the regionally averaged ensemble medians of the indices show various changes over different subregions. At 1.5 °C and 2 °C GWLs, most pronounced increases of threshold indices, i.e. summer days (SU) and tropical nights (TR), are projected in Sumatra and Sulawesi for both wet and dry seasons. The warm spell duration (WSDI) increases generally, with strongest magnitudes for Sumatra and Sulawesi (Philippines and Sulawesi) in the wet (dry) season. On the other hand, significant increases of warm days and nights can also be observed at 2 °C GWL compared to 1.5 °C, particularly in the dry season, suggesting the high sensitivity of temperature extremes over the SEA. The projected potentially conspicuous temperature extremes under global warming of 1.5 °C and 2 °C primarily concentrate on the densely populated coastal regions of the main islands, showing the necessity of restricting global warming to 1.5 °C aiming at the eradication and reduction of regional climate stress for the human system in the developing countries over the SEA.

Keywords Paris Agreement · Extreme temperature · Seasonal variation · Southeast Asia

✉ Fei Ge
figo@cuit.edu.cn

✉ Xiefei Zhi
zhi@nuist.edu.cn

Extended author information available on the last page of the article

1 Introduction

The 2003 European heat wave, the hottest record-breaking summer since 1500, caused over 70,000 deaths and a significant reduction in primary productivity (Luterbacher et al. 2004; Ciais et al. 2005; Robine et al. 2008). The extremely hot weather in summer 2010, with around 55,000 deaths and 15 billion dollars of economic loss in Russia (Barriopedro et al. 2011; Rahmstorf and Coumou 2011), is attributed to Greenhouse gas emissions and predicted to intensify and become more common in the future (Schar et al. 2004). A heavy heat wave in India and Pakistan from May to June 2015 resulted in 4100 deaths (WMO 2016). Even devastating forest fires are attributed to extreme heat events (Hudson et al. 2011). Among others, these events motivated the accelerated formulation of climate protection goals adopted in the 21st Conference of Parties (COP21) of the United Nations Framework Convention of Climate Change (UNFCCC) in 2015, also known as the Paris Agreement (UNFCCC 2015), with the central aim of keeping a global temperature rise in this century below 2 °C above pre-industrial level and to pursue efforts to limit the temperature increase even further to 1.5 °C.

Following the Paris Agreement, the Intergovernmental Panel on Climate Change (IPCC) Special Report on Global Warming of 1.5 °C (SR15) has been released on 6 October, 2018, which assesses the effects of global warming of 1.5 °C above pre-industrial levels and strengthens the global response to potential risks of climate change (IPCC 2018). With respect to another target of limiting the increase in the global mean annual surface air temperature (GMAT) to “well below 2 °C” in the Paris Agreement, it has also been reported that the climate consequences of a 2 °C world are far greater than that of 1.5 °C (Schleussner et al. 2017; Dosio and Fischer 2018; IPCC 2018).

In most cases, global warming is closely associated with increases of extremes, including both temperature and precipitation, severely impacting the human systems especially in less-developed countries (Zhou et al. 2014; Mitchell et al. 2016; Sillmann et al. 2017; IPCC 2018). Previous studies have pursued a lot of efforts to evaluate the projected extreme events on the globe (Dosio et al. 2018) and also for the majority of populated land regions (Ma et al. 2018; Nikulin et al. 2018; Warnatzsch and Reay 2019). However, with regard to Southeast Asia (SEA), an area characterized by relatively low resilience and adaptive capacity for most countries, there are limited studies quantitatively investigating temperature extremes of 1.5 °C and 2 °C global warming (Tangang et al. 2018; Ge et al. 2019b). In fact, the IPCC Fifth Assessment Report (AR5) has revealed that SEA has already been exposed to extreme events with higher frequency and intensity induced by the significant climate warming, which is even likely to continue in the future (IPCC 2013, 2014), with critical influences on the local water resources, food security, agricultural production etc. Taking the high vulnerability to the climate change together with the high popularity into consideration, the further projection for the SEA is explicitly crucial for the local governments to implement related adaptations and mitigations (Hoang et al. 2019; Tang 2019).

It is known that reliable projections are of great importance in evaluating climate change information and the mitigation and adaptation measures (Moss et al. 2010; Xie et al. 2015; Holden et al. 2018). There have been plenty of investigations on the climate change impacts using a set of global climate models (GCMs) driven by several representative concentration pathway (RCP) scenarios, such as models included in the Coupled Model Intercomparison Project 5 (CMIP5; Knutti et al. 2013). However, the GCMs are featured by deficiencies of relatively coarse spatial resolutions and physical parameterizations (Gu et al. 2018). Responding to the higher demand of climate information at the regional scales, regional climate models (RCMs) have been increasingly applied in the climate detections focusing on a region of interest (Giorgi et al. 2009). Accordingly, the Coordinated Regional

Downscaling Experiment (CORDEX; Jones et al. 2011) under the World Climate Research Programme (WCRP) has been carried out based on a series of state-of-the-art RCMs, aiming at advancing and coordinating the science and application of regional climate downscaling through global partnerships (Giorgi et al. 2012; Li et al. 2018). It provides a sufficient avenue for researchers and policymakers to find a better understanding of the regional climate change (Gutowski et al. 2016).

As mentioned above, in view of ensembles of climate models from worldwide frameworks such as CMIP5 and CORDEX, plenty of information regarding regional climate changes has been provided (Hulme 2016; Schleussner et al. 2016; Li et al. 2019; Warnatzsch and Reay 2019). Nevertheless, the results obtained are mostly based on the annual time scale. There is still information missing on the seasonal details of the local response to the global warming, particularly for the vulnerable areas and the areas with robust seasonal climate signals (Hasson et al. 2016), which cannot be ignored. Therefore, the present study intends to provide detailed information of future regional climate over SEA as well as the subregions, and to examine the seasonal conditions and the changing magnitudes of temperature extremes under global warming levels (GWLs) of 1.5 °C and 2 °C, which are policy-relevant for countries in this area. The orography of SEA is shown in Fig. 1, including the five subregions, i.e., Indochina Peninsula (ICP; 6°N–23°N, 95°E–110°E), Philippines (PH; 5°N–20°N, 118°E–130°E), Sumatra (SUM; 8°S–6°N, 95°E–108°E), Kalimantan (KAL; 4°S–6°N, 109°E–118°E), and Sulawesi (SUL; 6°S–3°N, 118°E–126°E).

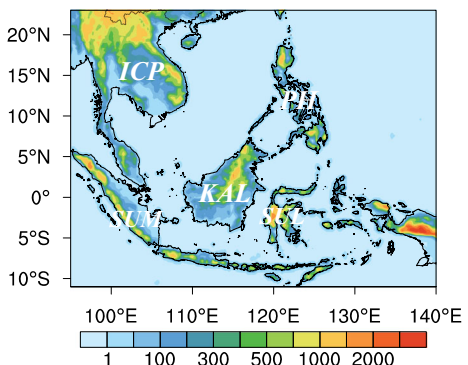
This paper is structured as follows. Section 2 briefly describes data from the models, reanalysis and the methods. In Section 3, we evaluate the performance of the used CORDEX RCMs. Afterwards, the projected temperature extremes in different seasons under the global warming of 1.5 °C and 2 °C are also analyzed in the same section. Finally, the summary and discussion are presented in Section 4.

2 Data and methods

2.1 Datasets

The data used in this study are derived from the current available CORDEX ensemble with the high resolution of 25 km. In the CORDEX framework (Giorgi and Gutowski 2015), the RCM runs initiated for both Southeast Asia and East Asia cover the SEA region, consisting of four

Fig. 1 The orography (Unit: m) of SEA and the geographical locations of the five subregions (ICP: Indochina Peninsula, 6°N–23°N, 95°E–110°E; PH: Philippines, 5°N–20°N, 118°E–130°E; SUM: Sumatra, 8°S–6°N, 95°E–108°E; KAL: Kalimantan, 4°S–6°N, 109°E–118°E; SUL: Sulawesi, 6°S–3°N, 118°E–126°E)



and six RCMs, respectively (Table 1) which, for the projection over the SEA, compose the ensemble of 10 models in total. Hereinafter, an individual model run is referred by the RCM followed by the parentheses with the corresponding driving GCM inside, e.g., RegCM4 (MPI-ESM-MR) represents the simulation from the regional model RegCM4 driven by the global model MPI-ESM-MR.

Additionally, in order to validate the historical simulations of the RCMs for the reference period of 1976–2005, the daily mean, maximum, and minimum temperatures from the CERA-20C, i.e., the ensemble of European Centre for Medium-Range Weather Forecasts (ECMWF) air-sea coupled climate reanalysis of the twentieth century (1901–2010), are taken as observations, which have been proved to be able to improve the representations of geophysical process for both atmosphere and ocean and to reconstruct the past weather and climate of the Earth system (Lalouaux et al. 2018). The CERA-20C reanalysis data are derived with a horizontal resolution of $0.25^\circ \times 0.25^\circ$ from the ECMWF data server at <https://apps.ecmwf.int/datasets/>.

2.2 Definition of the 1.5 °C and 2 °C GWLs

The GWL of a specific RCM dynamical downscaling is determined on the corresponding driving GCM from CMIP5. So far, several approaches have been involved to identify the GWL timing, which show only few differences (King et al. 2017; Chen and Sun 2018). In this study, we use 30-year time slices to eliminate the interannual climate variability and to represent a stabilized climate (Zhu et al. 2016). The pre-industrial climate is taken from 1881 to 1910, which is included in all CMIP5 historical simulations. First, a 30-year running mean is performed to smooth the time series of the GMAT from GCMs. Afterwards, the 30-year periods of the running means reaching 1.5 °C and 2 °C higher than the pre-industrial baseline are identified as the corresponding GWL tracking periods under the scenarios (for more information see Kjellström et al. 2018 and Nikulin et al. 2018). For instance, the CCLM5 (CNRM-CM5) model reaches its 1.5 °C and 2 °C GWLs at 2021–2050 and 2043–2072 under the RCP 4.5 scenario, and at 2015–2044 and 2030–2059 under the RCP 8.5 scenario,

Table 1 Brief information of the climate model simulations from CORDEX applied in this study

RCM		GCM		Model domain	Scenarios (RCP)
Model	Institution	Model	Institution		
RegCM4-3	ICTP, Italy	EC-EARTH	ICHEC, Netherlands/Ireland	SEA	4.5, 8.5
RCA4	SMHI, Sweden	HadGEM2-ES	MOHC, UK	SEA	4.5, 8.5
RegCM4-3	ICTP, Italy	IPSL-CM5A-LR	IPSL, France	SEA	4.5, 8.5
RegCM4-3	ICTP, Italy	MPI-ESM-MR	MPI-M, Germany	SEA	4.5, 8.5
HIRHAM5	DMI, Denmark	EC-EARTH	ICHEC, Netherlands/Ireland	EAS	4.5, 8.5
HadGEM3-RA	MOHC, UK	HadGEM2-AO	MOHC, UK	EAS	4.5, 8.5
CCLM5	CLMcom	CNRM-CM5	CERFACS, France	EAS	4.5, 8.5
CCLM5	CLMcom	EC-EARTH	ICHEC, Netherlands/Ireland	EAS	4.5, 8.5
CCLM5	CLMcom	HadGEM2-ES	MOHC, UK	EAS	4.5, 8.5
CCLM5	CLMcom	MPI-ESM-LR	MPI-M, Germany	EAS	4.5, 8.5

respectively. It is worth noting that a given year is allowed to contribute to both of the two GWLs, since we do not assume independence between the two GWL worlds (Bhownick et al. 2019).

It has been revealed that the GWL results are relatively independent to the RCP scenarios (King and Karoly 2017; Dosio and Fischer 2018), which illustrates that different RCP experiments do not vary a lot in temperature patterns at the same GWL for most parts of the world. Thus, aiming at the detection of future climate change over the SEA, there are 10 RCMs all assuming RCP 4.5 and 8.5, which overall present results from 20 ensemble members for each GWL. The climate warming consequences are presented as the differences between the GWLs and the historical 30-year reference period of 1976–2005.

2.3 Index representation of temperature extremes

A total of 27 indices characterizing climate and climate change are recommended by the World Meteorological Organization (WMO; Karl et al. 1999) and the Expert Team on Climate Change Detection and Indices (ETCCDI; Zhang et al. 2011; Sillmann et al. 2013a), including 16 for temperature extremes and 11 for precipitation extremes. However, they are not all applicable for regions with tropical climate features. Hence, eight of them (Table 2) are selected to quantify the temperature extremes over the SEA based on daily maximum and minimum of surface air temperature. More detailed information on the indices can be found at the ETCCDI website <http://etccdi.pacificclimate.org/indices.shtml>.

2.4 Model performance metrics

Confidence in climate projections depends on the adequacy of the climate models for these projections. The most common method of assessing a climate model is the quantitative assessment of “model-fit”; that is, how well the model results match observation-based data (empirical accuracy) and match other models or model versions (robustness). In this paper, we are using the metrics relative root mean square error (RMSE') and signal to noise ratio (SNR) to quantify the empirical accuracy and the robustness, respectively.

Given the large number of indices and models presented in the study, the relative error is applied to assess the model capability in climate simulation, which is represented by the RMSE' (Gleckler et al. 2008; Zhou et al. 2014; Dong et al. 2015) defined as follows. Firstly,

Table 2 The selected extreme temperature indices recommended by the ETCCDI. (TX daily maximum temperature; TN daily minimum temperature)

Index	Definition	Unit
SU	Number of summer days (TX > 25 °C).	day
TR	Number of tropical nights (TN > 20 °C).	day
WSDI	Warm spell duration index (number of the days summed by periods where at least 6 consecutive days when TX > the calendar day 90th percentile centered on a 5-day window for the base period 1961–1990).	day
DTR	Daily temperature range (difference between TX and TN).	°C
TXx	Monthly maximum value of TX.	°C
TNx	Monthly maximum value of TN.	°C
TXn	Monthly minimum value of TX.	°C
TNn	Monthly minimum value of TN	°C

the root mean squared error (RMSE) is calculated for each model index from an individual RCM relative to the CERA-20C observations:

$$\text{RMSE} = \sqrt{(X-Y)^2} \quad (1)$$

where X and Y are the temperature extreme indices derived from the model simulation and observation, respectively. All RMSEs are then used to derive the RMSE' of each model:

$$\text{RMSE}' = \frac{(\text{RMSE} - \text{RMSE}_{\text{Median}})}{\text{RMSE}_{\text{Median}}} \quad (2)$$

with $\text{RMSE}_{\text{Median}}$ being the ensemble median of all model RMSEs. Generally, a negative (positive) RMSE' of a model indicates that it has better (worse) performance than half of the total members.

Furthermore, the SNR is calculated to examine the credibility of projection results from the ensemble via the formula (Shi et al. 2018):

$$\text{SNR} = |x_e| / \sqrt{\frac{1}{n} \sum_{i=1}^n (x_i - x_e)^2} \quad (3)$$

where x_i represents the simulated index from a single model, x_e denotes the ensemble result, and n is the ensemble size. Therefore, $\text{SNR} > 1$ implies that the signal (numerator) is greater than the noise (denominator), indicating the considerable consistency and reliability of the projection.

In addition, all statistical significances are tested at the 95% confidence level by the two-tailed Student's t test. The consequences of global warming are presented as the differences between the climate over GWL periods and the historical reference period of 1976–2005.

In contrast to the four seasons in the Northern Hemisphere defined as spring (March–May), summer (June–August), autumn (September–November), and winter (December - subsequent February) and vice versa for the Southern Hemisphere, tropical areas experience a rainy season from April to September and a dry season from October to the subsequent March. Seasons defined as “wet season” and “dry season” are used in this study for the SEA (Nguyen et al. 2014; Villafuerte and Matsumoto 2015; Ge et al. 2017; Ge et al. 2019a).

3 Results

The results are presented in terms of (1) the assessment of CORDEX RCM simulated temperature extreme indices compared to observations, (2) the spatial patterns of projected changes of temperature extremes in wet and dry seasons for the 1.5 °C and 2 °C GWLs over the SEA, the regionally averaged temperature indices of the individual main islands are presented by box-and-whisker plots, and (3) the temperature extreme changes due to an additional 0.5 °C GWL between wet and dry seasons.

3.1 Evaluation for CORDEX RCMs

The RMSE' of individual models in simulating the temperature extremes compared with the CERA-20C observations are shown in Fig. 2. The results indicate that the model simulations differ to a great deal in the indices of SU (summer days), TR (tropical nights), WSDI (warm spell duration index),

and DTR (daily temperature range). As for the other four indices of TXx (monthly maximum value of daily maximum temperatures), TNx (monthly maximum value of daily minimum temperatures), TXn (monthly minimum value of daily maximum temperatures), and TNn (monthly minimum value of daily minimum temperatures), the model performances are similar, with their RMSE' ranging from -0.05 to 0.05. In general, HIRHAM5 (EC-EARTH) and RegCM4 (IPSL-CM5A-LR) simulate the indices fairly well in the wet season, while CCLM5 (EC-EARTH) and HIRHAM5 (EC-EARTH) show better results in the dry season. Relatively weak overall performances occur in simulations from CCLM5 (CNRM-CM5), CCLM5 (HadGEM2-ES), and CCLM5 (MPI-ESM-LR) in the wet season, whereas RegCM4 (IPSL-CM5A-LR) and CCLM5 (MPI-ESM-LR) perform poorly in the dry season, with positive RMSE' values for most indices. That is, the model performances differ not only for different indices but also in different seasons, which further confirms the necessity to investigate the model ensemble on the basis of eight indices and two seasons, respectively.

Thus, the RMSE' of the ensemble medians are shown in Fig. 2 (last row). In order to avoid the influences by abnormally large model errors (outliers), the model ensemble median is chosen to represent the deterministic ensemble result rather than the mean value. It is demonstrated from Fig. 2 that the ensemble median outperforms individual models for all indices in both wet and dry seasons, which diminishes the structural model uncertainties to a great extent. Therefore, the ensemble median can be considered to reasonably represent the future projections in the study.

3.2 Projected changes of temperature extremes in wet and dry seasons at 1.5 °C and 2 °C GWLs

The seasonal spatial distributions of projected changes of ensemble medians in extreme temperature indices over the SEA at the 1.5 °C and 2 °C GWLs are presented in Figs. 3 and 4. In both wet and dry seasons at the 1.5 °C GWL (Fig. 3), the indices are projected to significantly increase across ICP and Maritime Continent, except DTR. It is noteworthy that the projected changes indicate prominent increases with disproportionately large spatial extents

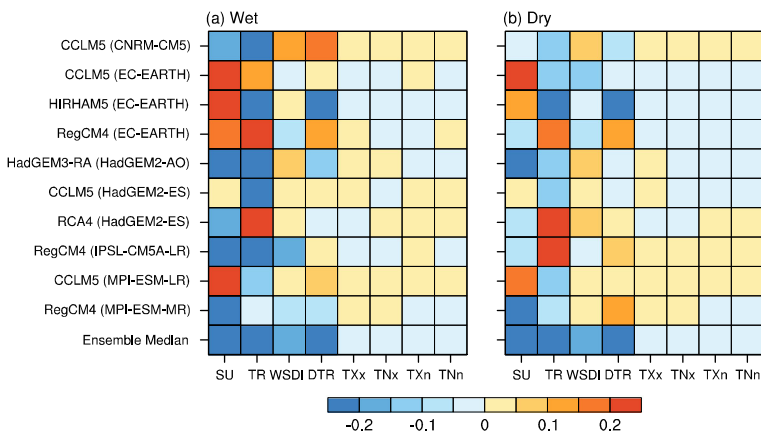


Fig. 2 Raster diagrams of the relative RMSEs (RMSE') of extreme temperature indices simulated by CORDEX models versus the observation during the period of 1976–2005 for **a** wet and **b** dry seasons. The labels at the X-axis denote the used extreme indices, which are introduced in Table 2. The labels at the Y-axis represent the specific model runs, referred by the RCM followed by its corresponding driving GCM in the parentheses

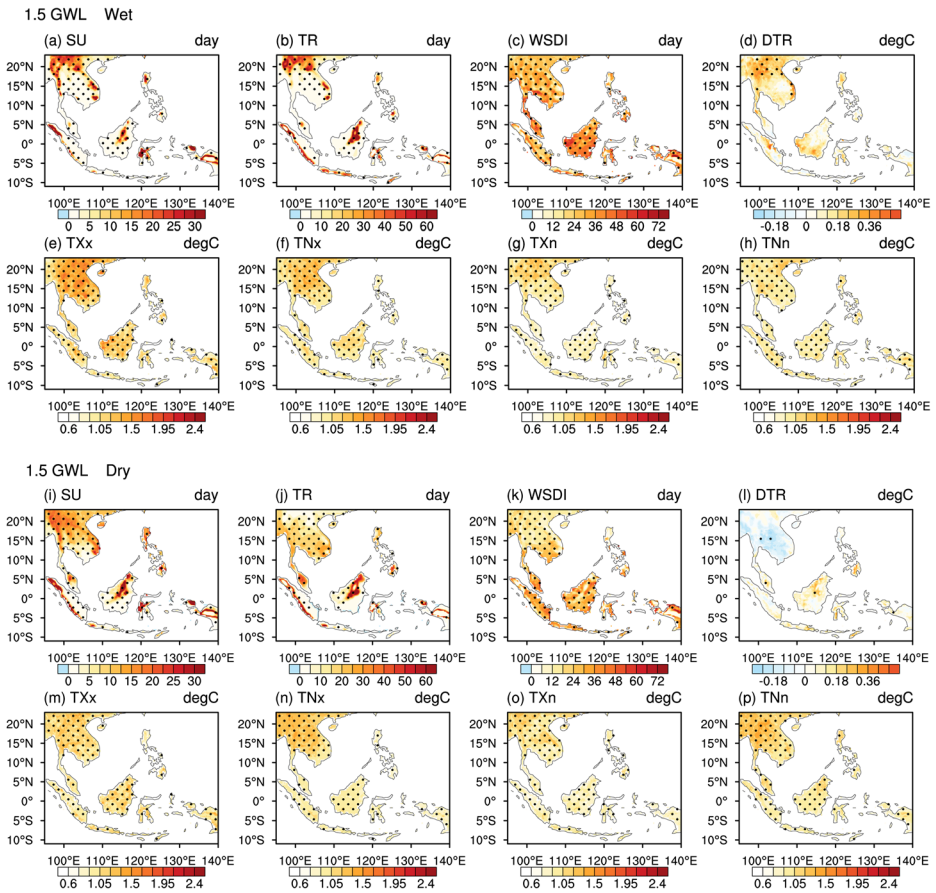


Fig. 3 Projected CORDEX ensemble median changes in extreme temperature indices at the 1.5 °C GWL relative to 1976–2005 for wet (a–h) and dry (i–p) seasons. The black dots indicate statistical significance at the 95% confidence level. All SNRs are greater than 1 over the area

and magnitudes in the ICP and KAL at the 2 °C GWL compared to the 1.5 °C GWL in both wet and dry seasons (Fig. 4).

Abnormal decreases of DTR mainly appear over the central areas of ICP in the dry season for both GWLs (Figs. 3l and 4l). Conversely, it shows partially significant increases over the northern mountainous areas of ICP in the wet season (Figs. 3d and 4d). DTR is always considered a useful index of global and local climate change, which could be explained by inconsistent rapid increase of maximum and minimum temperatures (Easterling et al. 1997; Braganza et al. 2004; Vose et al. 2005; Alexander and Arblaster 2009; Yao et al. 2013). Reduced DTR in the dry season occurs mainly over the central and coastal ICP, while the increased DTR in the wet season concentrates in the mountainous northern ICP and the Southwest KAL, which resembles the results extracted from the model simulations and projections in CMIP5 (Lewis and Karoly 2013; Lindvall and Svensson 2015).

On the other hand, SU and TR indicate consistent increases in both seasons at 1.5 °C and 2 °C GWLs over the whole ICP and Maritime Continent. The four indices of TXx, TXn, TNx, and TNn, which are simply derived from maximum and minimum temperatures, are projected to increase constantly in wet and dry seasons over SEA at 1.5 °C and 2 °C GWLs. The

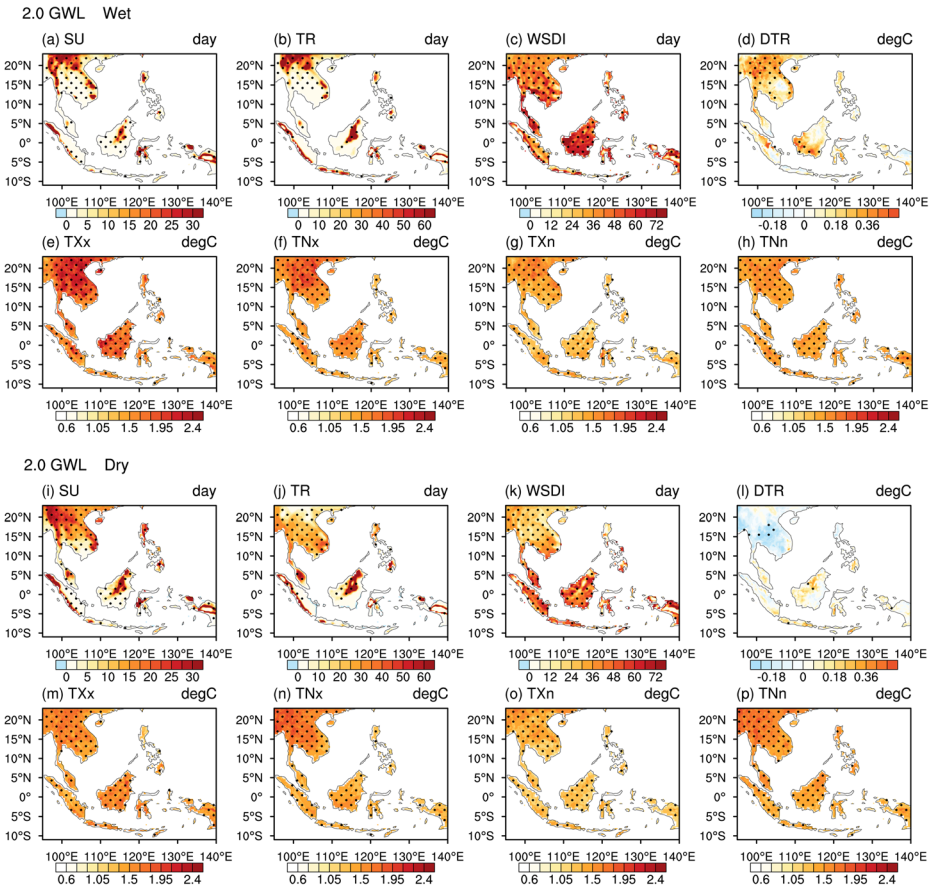


Fig. 4 Same as Fig. 3, but at the 2.0 °C GWL

increased WSDI implies the warm spell duration to become longer over SEA, especially at the 2 °C GWL. Generally, the results suggest that the temperature extremes would establish in both seasons at both 1.5 °C and 2 °C GWLs. This is likely to have potential negative impacts on human systems in the developing countries with large coastal population densities in the ICP and Maritime Continent.

El Niño–Southern Oscillation (ENSO) could also modulate the extreme events over the SEA: The numbers of warm days and warm nights, which are closely associated with the daily maximum and minimum temperatures increase substantially during the El Niño decaying year, whereas the cool days and cold nights are significantly decreasing (Manton et al. 2001; Nicholls et al. 2005). Moreover, the change of nighttime warming exceeding that of daytime occurs over the most of ICP during the recent several decades (Marjuki et al. 2016). Lately, it has been reported that the extreme drought over the ICP in April 2016 is predominately caused by the super El Niño event during 2015–2016. ENSO events would occur more frequently under the continuous global warming in the future, which, in turn, brings more record-breaking surface air temperatures over the SEA (Thirumalai et al. 2017; Lehner et al. 2018).

During the dry season, the decreased DTR over the ICP could be related to the changes of surface air temperatures associated with El Niño events and the enhanced greenhouse gases

(Zhou et al. 2010), which is also consistent with our results of an increasing number of summer days (SU) and tropical nights (TR). During the wet season, larger high-confidence area of increasing TXx can be observed under the two GWLs compared with that during the dry season, while the magnitude of increasing TNn is lower than that in the dry season. This suggests the range between daily maximum and minimum temperatures, which is the DTR, to be larger. In addition, precipitation also plays a crucial role in DTR changes over the tropics (Portmann et al. 2009). Significantly amplified convective precipitation over the ICP and Maritime Continent in the rainy season at 1.5 °C and 2 °C GWLs tends to suppress an increasing of daily minimum temperature and thus to favor DTR increase (Zhou et al. 2009; Ge et al. 2019b). Explanations of the projected DTR changes have been provided in previous studies, which reveal that DTR is affected by plenty of processes and its change cannot be attributed to a single parameter. That is, which of the possible underlying mechanisms, such as cloudiness, water vapor content, and atmospheric stratification, is dominant depends on the regional climatological setting and still requires further examination in the future.

To identify the detailed climate response to the two GWLs in wet and dry seasons, projected percentage changes of the indices averaged over each subregion over the SEA are presented in the boxplots of Figs. 5 and 6. In general, threshold indices (SU and TR) and duration indices (WSDI) indicate distinctly larger spreads than the other ones simply derived from the daily maximum and minimum temperatures. However, it is noted that the ensemble medians of the index changes are all greater than 0 except DTR, which implies increasing trends of temperature extremes compared to the reference period of 1976–2005.

The more pronounced increases of SU are projected in the dry season compared to the wet season, while it shows the reversed case for SUL. TR, based on the fixed 20 °C threshold for the nighttime, increases robustly for all subregions, especially over ICP and SUL in the dry season with the percentage magnitudes of 93.5% and 97.1% (150.4% and 239.4%), respectively, at the 1.5 °C (2 °C) GWL. It is implied that almost the entire area will be characterized by nighttime temperatures above 20 °C at the 2 °C GWL, suggesting the critical long-term warming in the SEA if the warming continues. Besides, as for the WSDI index, the most pronounced increases can be found over SUM and SUL in the wet season at the 2 °C GWL with the magnitudes of 165.1% and 203.9%. Over PH and KAL, the strong increases of WSDI mainly occur in the dry season. Actually, WSDI is revealed by previous studies (Sillmann et al. 2013b) to be more sensitive to the magnitude of maximum temperature changes, especially in tropical regions with the low short-term tropical temperature variability.

According to projected changes in the absolute temperature values (TX and TN), it exactly shows relatively low variation at 1.5 °C and 2 °C GWLs over the SEA, which corresponds well with the results described above. But even for slight changes of the maximum and minimum temperatures between 1.5 °C and 2 °C GWLs, the climate impacts over the SEA could be huge. In addition, the projected percentage changes feature relatively large ensemble spreads for all the indices at the 2 °C GWL, which is probably due to the stronger regional land-atmosphere feedbacks and larger differences between the models at the higher GWL.

3.3 Differences of temperature extremes between 1.5 °C and 2 °C GWLs for the two seasons

The differences between 2 °C and 1.5 °C GWL in each season are shown in Fig. 7 to investigate the potential impacts of the additional 0.5 °C GWL over the SEA, as well as their seasonal differences in Fig. 8.

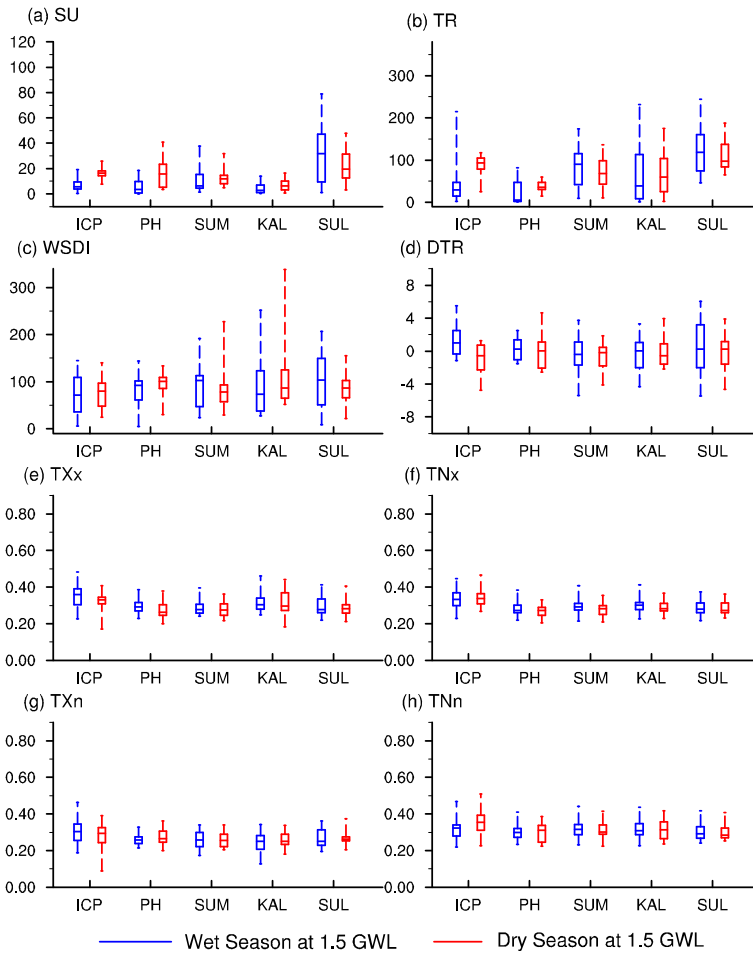


Fig. 5 Boxplot of the projected percentage changes of temperature extreme indices averaged over each subregion of SEA at the 1.5 °C GWL relative to 1976–2005 for wet (blue) and dry (red) seasons. Boxes indicate the interquartile model spread (25th and 75th quantiles) with the horizontal line indicating the ensemble median and the whiskers showing the extreme range of the ensemble

It is clearly indicated that the regional ensemble median changes of threshold indices (SU and TR) reveal general increases over most areas of ICP and Maritime Continent in either wet or dry seasons. Besides, they are mainly characterized by negative differences between wet and dry seasons (Fig. 8a, b), indicating more pronounced changes of SU and TR in the dry season. That is, more warm days and nights are expected in the dry season compared with the wet season due to the additional 0.5 °C GWL. WSDI changes are projected to increase constantly over the whole SEA in both seasons (Fig. 7c, k), with the seasonal differences mainly positive over ICP and central KAL, suggesting the higher sensitivity of WSDI changes in the wet season. On the other hand, DTR changes induced by the additional 0.5 °C GWL show opposite patterns between wet and dry seasons, although most of them are not significant.

Corresponding to the additional GWL of 0.5 °C, the absolute indices of TXx, TNx, TXn, and TNn show general increasing trends over the whole SEA, with relatively higher magnitudes in TXx and TNx than the other two indices. It is also notable that their changes are

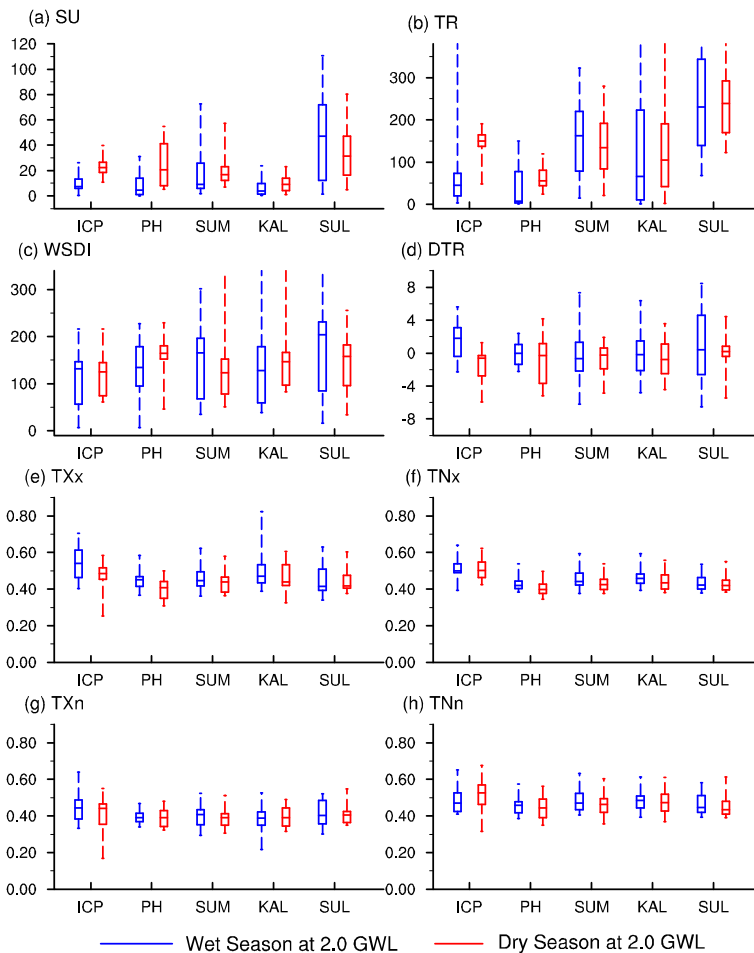


Fig. 6 Same as Fig. 5, but at the 2.0 °C GWL

extensively greater in the wet season than in the dry season over the SEA especially ICP because of the warmer globe of 0.5 °C, which are consistent with the spatial patterns in Figs. 3 and 4. In general, the temperature extremes would be characterized by higher intensity and longer duration as a response to the additional 0.5 °C GWL. It would also have potential influences on growing crops, especially for the growth of rice seedling during the wet season. Additionally, these results also indicate that changes of the ensemble median temperature extreme indices vary independently over the SEA, suggesting a region- and season-dependent high sensitivity of heat stress to the additional 0.5 °C GWL.

4 Conclusions and discussion

In this study, the projected changes in temperature extremes at 1.5 °C and 2 °C global warming levels (GWLs) have been evaluated for Southeast Asia (SEA) based on temperature extreme indices from ETCCDI (Table 2) using the latest available CORDEX simulations. For the first

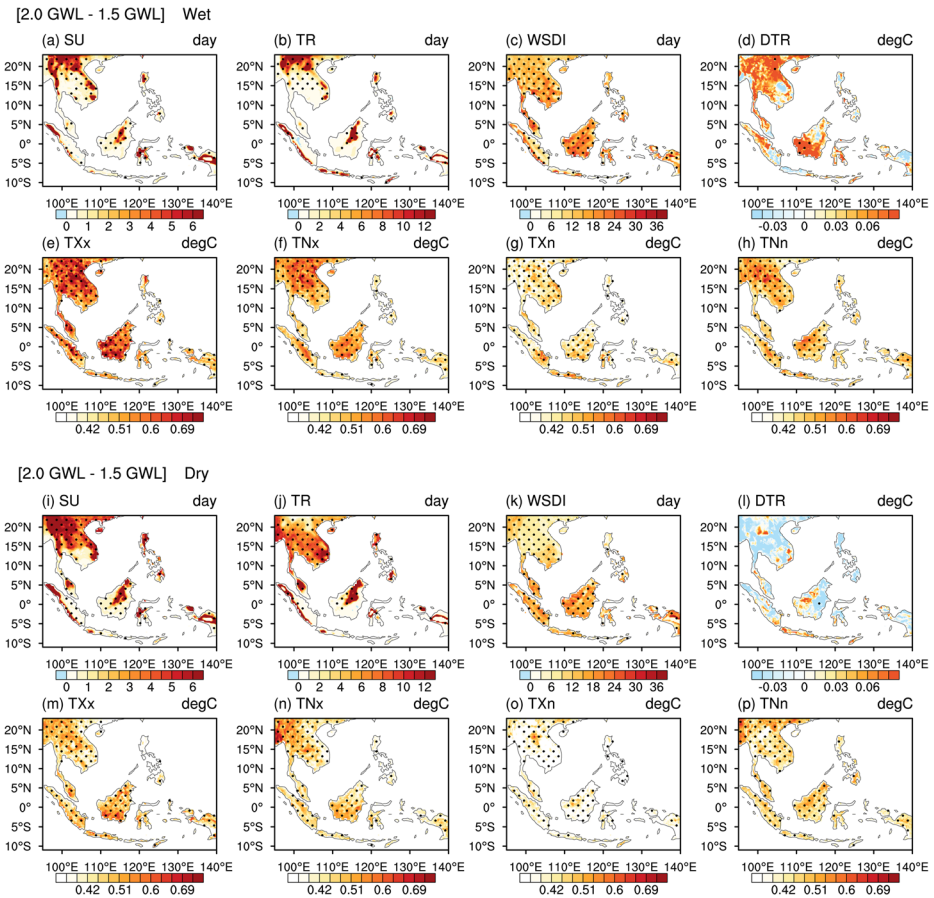


Fig. 7 Differences between the ensemble median changes of extreme temperature indices at the 1.5 °C and 2 °C GWL in wet (a–h) and dry (i–p) seasons. The black dots indicate statistical significance at the 95% confidence level. All SNRs are greater than 1 over the area

time, the results provide detailed information on the future climate changes expected for the subregions in the SEA, with the frequency and intensity of temperature extremes being strengthened in wet and dry seasons under the global warming conditions guided by the Paris Agreement. The main findings are summarized as follows:

1. The ensemble medians of temperature indices show significant increases across ICP and Maritime Continent at 1.5 °C and 2 °C GWLs except for the decreasing DTR in the dry season. Additionally, predominant changes in most of the indices are more significant at the 2 °C GWL than at the 1.5 °C GWL, while seasonal differences of the changes mainly concentrate on the four indices of SU, TR, WSDI, and DTR.
2. The regionally averaged medians of the indices show various changes over different subregions. At both GWLs, the most pronounced increases of SU are projected in SUL with the percentage magnitude of 31.7% and 19.7% (47.2% and 31.3%) at the 1.5 °C (2 °C) GWL for wet and dry seasons, respectively, while TR increases robustly over SUM and SUL. The warm spell duration (WSDI) increases generally, with strongest magnitudes

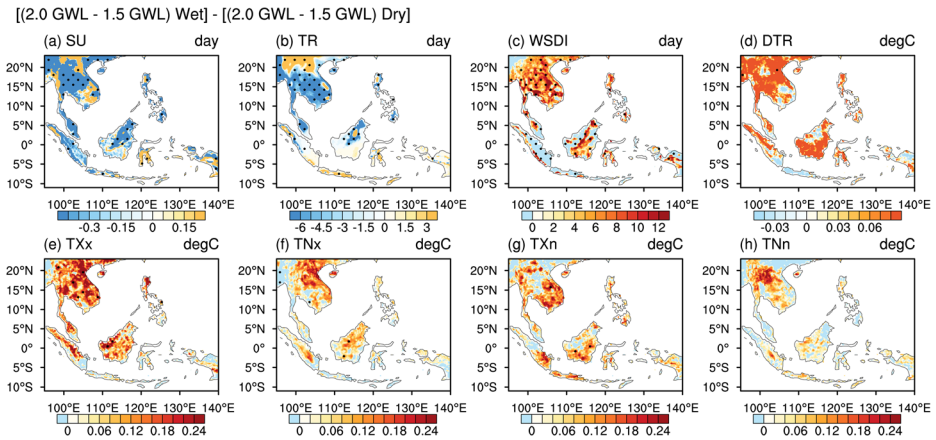


Fig. 8 Differences between the wet and dry seasons for the extreme temperature index changes due to the additional 0.5 °C GWL. The black dots indicate statistical significance at the 95% confidence level. All SNRs are greater than 1 over the area

for SUM and SUL (PH and SUL) in the wet (dry) season. On the other hand, projected changes in the absolute indices (TX and TN) are featured by lower variations at 1.5 °C and 2 °C GWLs over SEA.

- Robust differences of temperature extremes can be found over the SEA in both wet and dry seasons for the additional global warming of 0.5 °C. The most pronounced increases for the threshold indices (SU and TR) appear in the dry season over ICP at the 2 °C GWL compared to the lower one. WSDI is projected to increase consistently over the whole SEA in both seasons, while DTR shows non-significant increase and decrease tendencies in wet and dry seasons, respectively. The changes of absolute indices (TX and TN) are generally greater due to the warmer future climate at the 2 °C GWL. Therefore, more warm days and nights are expected due to the additional 0.5 °C warming, particularly in the dry season. The temperature extremes under the global warming of 1.5 °C and 2 °C levels as well as their differences mainly concentrate on the main islands in the densely populated coastal regions, suggesting more conspicuous impacts on the human system in the less-developed countries over the SEA.

In the context of strengthening the global response to the potential threat of climate change, the IPCC SR15 has pointed out that limiting warming to 1.5 °C is already barely feasible, but the window of opportunity is not yet closed, which is a wake-up call about the huge challenges induced by the escalating threats from rising temperatures. For the SEA, where it is highly vulnerable to the climate change due to the complex orography and the relatively fragile human system, the climate stress under the global warming could never be ignored (Liobikienė and Butkus 2018). It has been noticed that several studies have been carried out to project the precipitation extremes over the SEA at different GWLs (Tangang et al. 2018; Ge et al. 2019b), which further inspires the present investigation on the potential temperature extremes over the SEA, indicating the necessity of restricting global warming on the eradication and reduction of regional climate extreme events.

Climate change risks should not only be considered in terms of the occurrence probability of extreme events, but should also include population exposure and local vulnerability (Chen and Sun 2019) which, in addition, vary across temporal and spatial scales and depend on economy, sociality, geography, demography, culture, and governance (IPCC 2012, 2018). Climate change is reported to

pose generally profound threats on public health (Wang et al. 2019), energy supply (Cortekar and Groth 2015), agriculture (Naylor et al. 2007), wildfire (Sun et al. 2019b), and many other factors. Although different RCP scenarios generally do not vary a lot on projected extreme patterns, abnormal characteristics might occur with hotspots over specific areas (Shi et al. 2018). To promote sustainable development on human systems under constant global warming, more complex aspects are still on the way to be addressed such as to what extent do anthropogenic activities attribute to the climate change over SEA (Marotzke et al. 2017; Cai et al. 2019). Additionally, considering the intrinsic model characteristics, more work remains to be carried out regarding comparisons between model ensembles with and without bias correction, as well as among multiple bias correction methods (Maraun et al. 2017; Guo et al. 2018; Sun et al. 2019a). More well-developed climate models including both GCMs and RCMs are also of great importance in the ongoing future analysis on climate change.

Acknowledgments Three anonymous reviewers are thanked for their constructive comments that greatly improved the quality of the manuscript. We are grateful to WCRP CORDEX, ECMWF, ETCCDI, the German Climate Computing Center (DKRZ) and the climate modeling groups (listed in Table 1) for their data and resources.

Funding information Joint financial support provided by the National Key R&D Program of China (Grant Nos. 2017YFC1502002, 2018YFC1505702, and 2018YFC1506104), the National Natural Science Foundation of China (Grant Nos. 41805056 and 41776002), the Strategic Priority Research Program of Chinese Academy of Sciences (Grant No. XDA20060501), the Program for Professor of Special Appointment (Eastern Scholar) at Shanghai Institutions of Higher Learning (A1-2048-18-0001), the Postgraduate Research & Practice Innovation Program of Jiangsu Province (Grant No. KYCX17_0875), the Scientific Research Fund of Sichuan Provincial Education Department (18ZB0112), the Open Research Fund Program of KLME, NUIST (KLME201809), and the China Scholarship Council (Grant Nos. 201808510009 and 201608320193).

References

- Alexander LV, Arblaster JM (2009) Assessing trends in observed and modelled climate extremes over Australia in relation to future projections. *Int J Climatol* 29:417–435
- Barriopedro D, Fischer EM, Luterbacher J et al (2011) The hot summer of 2010: redrawing the temperature record map of Europe. *Science* 332:220–224
- Bhowmick M, Sahany S, Mishra SK (2019) Projected precipitation changes over the south Asian region for every 0.5° C increase in global warming. *Environ Res Lett* 14:054005
- Braganza K, Karoly DJ, Arblaster JM (2004) Diurnal temperature range as an index of global climate change during the twentieth century. *Geophys Res Lett* 31:L13217
- Cai D, Fraedrich K, Guan Y et al (2019) Urbanization and climate change: insights from eco-hydrological diagnostics. *Sci Total Environ* 647:29–36
- Chen H, Sun J (2018) Projected changes in climate extremes in China in a 1.5 °C warmer world. *Int J Climatol* 38:3607–3617
- Chen H, Sun J (2019) Increased population exposure to extreme droughts in China due to 0.5°C of additional warming. *Environ Res Lett*. <https://doi.org/10.1088/1748-9326/ab072e>
- Ciais P, Reichstein M, Viovy N et al (2005) Europe-wide reduction in primary productivity caused by the heat and drought in 2003. *Nature* 437:529–533
- Cortekar J, Groth M (2015) Adapting energy infrastructure to climate change – is there a need for government interventions and legal obligations within the German “Energiewende”? *Energy Procedia* 73:12–17
- Dong S, Xu Y, Zhou B et al (2015) Assessment of indices of temperature extremes simulated by multiple CMIP5 models over China. *Adv Atmos Sci* 32:1077–1091
- Dosio A, Fischer EM (2018) Will half a degree make a difference? Robust projections of indices of mean and extreme climate in Europe under 1.5 °C, 2 °C, and 3 °C global warming. *Geophys Res Lett* 45:935–944
- Dosio A, Mentaschi L, Fischer EM et al (2018) Extreme heat waves under 1.5° C and 2° C global warming. *Environ Res Lett* 13:054006

- Easterling DR, Horton B, Jones PD et al (1997) Maximum and minimum temperature trends for the globe. *Science* 277:364–367
- Ge F, Zhi X, Babar Z et al (2017) Interannual variability of summer monsoon precipitation over the Indochina peninsula in association with ENSO. *Theor Appl Climatol* 128:523–531
- Ge F, Peng T, Fraedrich K et al (2019a) Assessment of trends and variability in surface air temperature on multiple high-resolution datasets over the Indochina peninsula. *Theor Appl Climatol* 135(3–4):1609–1627
- Ge F, Zhu S, Peng T et al (2019b) Risks of precipitation extremes over Southeast Asia: does 1.5°C or 2°C global warming make a difference? *Environ Res Lett* 14:044015
- Giorgi F, Gutowski WJ (2015) Regional dynamical downscaling and the CORDEX initiative. *Annu Rev Environ Resour* 40:467–490
- Giorgi F, Jones C, Asrar GR (2009) Addressing climate information needs at the regional level: the CORDEX framework. *World Meteorological Organization (WMO) Bulletin* 58:175–183
- Giorgi F, Coppola E, Solmon F et al (2012) RegCM4: model description and preliminary tests over multiple CORDEX domains. *Clim Res* 52:7–29
- Gu H, Yu Z, Yang C et al (2018) High-resolution ensemble projections and uncertainty assessment of regional climate change over China in CORDEX East Asia. *Hydrol Earth Syst Sci* 22:3087–3103. <https://doi.org/10.5194/hess-22-3087-2018>
- Guo L, Gao Q, Jiang Z et al (2018) Bias correction and projection of surface air temperature in LMDZ multiple simulation over central and eastern China. *Adv Clim Change Res* 9:81–92
- Gutowski WJ Jr, Giorgi F, Timbal B et al (2016) WCRP coordinated regional downscaling experiment (CORDEX): a diagnostic MIP for CMIP6. *Geosci Model Dev* 9:4087–4095
- Hasson S, Pascale S, Lucarini V et al (2016) Seasonal cycle of precipitation over major river basins in south and Southeast Asia: a review of the CMIP5 climate models data for present climate and future climate projections. *Atmos Res* 180:42–63
- Hoang LP, van Vliet MTH, Kummerow M et al (2019) The Mekong's future flows under multiple drivers: how climate change, hydropower developments and irrigation expansions drive hydrological changes. *Sci Total Environ* 649:601–609
- Holden PB, Edwards NR, Ridgwell A et al (2018) Climate–carbon cycle uncertainties and the Paris agreement. *Nat Clim Chang* 8:609–613. <https://doi.org/10.1038/s41558-018-0197-7>
- Hudson D, Marshall AG, Alves O (2011) Intraseasonal forecasting of the 2009 summer and winter Australian heat waves using POAMA. *Wea Forecasting* 26:257–279
- Hulme M (2016) 1.5 °C and climate research after the Paris agreement. *Nat Clim Chang* 6:222–224. <https://doi.org/10.1038/nclimate2939>
- IPCC (2012) Managing the risks of extreme events and disasters to advance climate change adaptation. A special report of working groups I and II of the intergovernmental panel on climate change. Cambridge University Press, Cambridge
- IPCC (2013) Climate change 2013: the physical science basis. Contribution of working group I to the Fifth Assessment Report of the Intergovernmental Panel on Climate Change. Cambridge University Press, Cambridge
- IPCC (2014) Climate change 2014: impacts, adaptation, and vulnerability. Part B: regional aspects. Contribution of working group II to the Fifth Assessment Report of the Intergovernmental Panel on Climate Change. Cambridge University Press, Cambridge, United Kingdom and New York, NY, USA
- IPCC (2018) Global warming of 1.5 °C, an IPCC special report on the impacts of global warming of 1.5°C above pre-industrial levels and related global greenhouse gas emission pathways, in the context of strengthening the global response to the threat of climate change, sustainable development, and efforts to eradicate poverty. World Meteorological Organization, Geneva, Switzerland
- Jones C, Giorgi F, Asrar G (2011) The coordinated regional downscaling experiment: CORDEX—an international downscaling link to CMIP5. *CLIVAR exchanges* 16:34–40
- Karl TR, Nicholls N, Ghazi A (1999) CLIVAR/GCOS/WMO workshop on indices and indicators for climate extremes: workshop summary. *Clim Chang* 42:3–7
- King AD, Karoly DJ (2017) Climate extremes in Europe at 1.5 and 2 degrees of global warming. *Environ Res Lett* 12:114031. <https://doi.org/10.1088/1748-9326/aa8e2c>
- King AD, Karoly DJ, Henley BJ (2017) Australian climate extremes at 1.5 °C and 2 °C of global warming. *Nat Clim Chang* 7:412–416
- Kjellström E, Nikulin G, Strandberg G et al (2018) European climate change at global mean temperature increases of 1.5 and 2 °C above pre-industrial conditions as simulated by the EURO-CORDEX regional climate models. *Earth Syst Dyn* 9:459–478
- Knutti R, Masson D, Gettelman A (2013) Climate model genealogy: generation CMIP5 and how we got there. *Geophys Res Lett* 40:1194–1199

- Lalouaux P, Boisseson E, Balmaseda M et al (2018) CERA-20C: a coupled reanalysis of the twentieth century. *J Adv Model Earth Syst* 10:1172–1195
- Lehner F, Deser C, Sanderson BM (2018) Future risk of record-breaking summer temperatures and its mitigation. *Clim Chang* 146:363–375
- Lewis SC, Karoly DJ (2013) Evaluation of historical diurnal temperature range trends in CMIP5 models. *J Clim* 26:9077–9089. <https://doi.org/10.1175/JCLI-D-13-00032.1>
- Li H, Chen H, Wang H et al (2018) Future precipitation changes over China under 1.5° C and 2.0° C global warming targets by using CORDEX regional climate models. *Sci Total Environ* 640:543–554. <https://doi.org/10.1016/j.scitotenv.2018.05.324>
- Li Y, Tao H, Su B et al (2019) Impacts of 1.5° C and 2° C global warming on winter snow depth in Central Asia. *Sci Total Environ* 651:2866–2873
- Lindvall J, Svensson G (2015) The diurnal temperature range in the CMIP5 models. *Clim Dyn* 44:405–421. <https://doi.org/10.1007/s00382-014-2144-2>
- Liobikiéné G, Butkus M (2018) The challenges and opportunities of climate change policy under different stages of economic development. *Sci Total Environ* 642:999–1007
- Luterbacher J, Dietrich D, Xoplaki E et al (2004) European seasonal and annual temperature variability, trends, and extremes since 1500. *Science* 303:1499–1503
- Ma X, Zhao C, Tao H et al (2018) Projections of actual evapotranspiration under the 1.5° C and 2.0° C global warming scenarios in sandy areas in northern China. *Sci Total Environ* 645:1496–1508. <https://doi.org/10.1016/j.scitotenv.2018.07.253>
- Manton MJ, Della-Marta PM, Haylock MR et al (2001) Trends in extreme daily rainfall and temperature in Southeast Asia and the South Pacific: 1961–1998. *Int J Climatol* 21:269–284
- Maraun D, Shepherd TG, Widmann M et al (2017) Towards process-informed bias correction of climate change simulations. *Nat Clim Chang* 7:764–773
- Marjuki, Van Der Schrier G, Klein Tank AMG et al (2016) Observed trends and variability in climate indices relevant for crop yields in Southeast Asia. *J Clim* 29:2651–2669
- Marotzke J, Jakob C, Bony S et al (2017) Climate research must sharpen its view. *Nat Clim Chang* 7:89–91
- Mitchell D, James R, Forster PM et al (2016) Realizing the impacts of a 1.5°C warmer world. *Nat Clim Chang* 6:735–737
- Moss RH, Edmonds JA, Hibbard KA et al (2010) The next generation of scenarios for climate change research and assessment. *Nature* 463:747–756
- Naylor RL, Battisti DS, Vimont DJ et al (2007) Assessing risks of climate variability and climate change for Indonesian rice agriculture. *Proc Natl Acad Sci U S A* 104:7752–7757
- Nguyen DQ, Renwick J, McGregor J (2014) Variations of surface temperature and rainfall in Vietnam from 1971 to 2010. *Int J Climatol* 34:249–264
- Nicholls N, Baek HJ, Gosai A et al (2005) The El Niño–southern oscillation and daily temperature extremes in East Asia and the West Pacific. *Geophys Res Lett* 32:L16714
- Nikulin G, Lennard C, Dosio A et al (2018) The effects of 1.5 and 2 degrees of global warming on Africa in the CORDEX ensemble. *Environ Res Lett* 13:065003
- Portmann RW, Solomon S, Hegerl GC (2009) Spatial and seasonal patterns in climate change, temperatures, and precipitation across the United States. *Proc Natl Acad Sci U S A* 106:7324–7329
- Rahmstorf S, Coumou D (2011) Increase of extreme events in a warming world. *Proc Natl Acad Sci U S A* 108:17905–17909
- Robine JM, Cheung SLK, Roy L et al (2008) Death toll exceeded 70,000 in Europe during the summer of 2003. *C R Biol* 331:171–178
- Schar C, Vidale PL, Luthi D et al (2004) The role of increasing temperature variability in European summer heatwaves. *Nature* 427:332–336
- Schleussner CF, Lissner TK, Fischer EM et al (2016) Differential climate impacts for policy-relevant limits to global warming: the case of 1.5 °C and 2 °C. *Earth Syst Dyn* 7:327–351
- Schleussner CF, Pfleiderer P, Fischer EM (2017) In the observational record half a degree matters. *Nat Clim Chang* 7:460–462
- Shi C, Jiang Z, Chen W et al (2018) Changes in temperature extremes over China under 1.5° C and 2° C global warming targets. *Adv Clim Change Res* 9:120–129
- Sillmann J, Kharin VV, Zhang X et al (2013a) Climate extremes indices in the CMIP5 multimodel ensemble: part 1. Model evaluation in the present climate. *J Geophys Res* 118:1716–1733
- Sillmann J, Kharin VV, Zwiers FW et al (2013b) Climate extremes indices in the CMIP5 multimodel ensemble: part 2. Future climate projections. *J Geophys Res* 118:2473–2493
- Sillmann J, Stjern CW, Myhre G et al (2017) Slow and fast responses of mean and extreme precipitation to different forcing in CMIP5 simulations. *Geophys Res Lett* 44:6383–6390
- Sun C, Jiang Z, Li W et al (2019a) Changes in extreme temperature over China when global warming stabilized at 1.5°C and 2.0°C. *Sci Rep* 9:14982

- Sun Q, Miao C, Hanel M et al (2019b) Global heat stress on health, wildfires, and agricultural crops under different levels of climate warming. *Environ Int* 128:125–136
- Tang KHD (2019) Climate change in Malaysia: trends, contributors, impacts, mitigation and adaptations. *Sci Total Environ* 650:1858–1871. <https://doi.org/10.1016/j.scitotenv.2018.09.316>
- Tangang F, Supari S, Chung JX et al (2018) Future changes in annual precipitation extremes over Southeast Asia under global warming of 2°C. *APN Sci Bul* 8:3–8
- Thirumalai K, DiNezio PN, Okumura Y et al (2017) Extreme temperatures in Southeast Asia caused by El Niño and worsened by global warming. *Nat Commun* 8:15531
- UNFCCC (2015) Adoption of the Paris agreement. I: proposal by the president (draft decision). United Nations Office, Geneva
- Villafuerte MQ, Matsumoto J (2015) Significant influences of global mean temperature and ENSO on extreme rainfall in Southeast Asia. *J Clim* 28:1905–1919
- Vose RS, Easterling DR, Gleason B (2005) Maximum and minimum temperature trends for the globe: an update through 2004. *Geophys Res Lett* 32:L23822
- Wang Y, Wang A, Zhai J et al (2019) Tens of thousands additional deaths annually in cities of China between 1.5°C and 2.0°C warming. *Nat Commun* 10:3376
- Wamatzsch EA, Reay DS (2019) Temperature and precipitation change in Malawi: evaluation of CORDEX-Africa climate simulations for climate change impact assessments and adaptation planning. *Sci Total Environ* 654:378–392. <https://doi.org/10.1016/j.scitotenv.2018.11.098>
- WMO (2016) WMO Statement on the Status of the Global Climate in 2015. Communication and Public Affairs Office, World Meteorological Organization, Geneva
- Xie SP, Deser C, Vecchi G et al (2015) Towards predictive understanding of regional climate change. *Nat Clim Chang* 5:921–930. <https://doi.org/10.1038/nclimate2689>
- Yao Y, Luo Y, Huang J et al (2013) Comparison of monthly temperature extremes simulated by CMIP3 and CMIP5 models. *J Clim* 26:7692–7707. <https://doi.org/10.1175/JCLI-D-12-00560.1>
- Zhang X, Alexander L, Hegerl GC et al (2011) Indices for monitoring changes in extremes based on daily temperature and precipitation data. *Wiley Interdiscip Rev Clim Chang* 2:851–870
- Zhou L, Dai A, Dai Y et al (2009) Spatial dependence of diurnal temperature range trends on precipitation from 1950 to 2004. *Clim Dyn* 32:429–440
- Zhou L, Dickinson RE, Dai A et al (2010) Detection and attribution of anthropogenic forcing to diurnal temperature range changes from 1950 to 1999: comparing multi-model simulations with observations. *Clim Dyn* 35:1289–1307
- Zhou B, Han WQZ, Xu Y et al (2014) Projected changes in temperature and precipitation extremes in China by the CMIP5 multimodel ensembles. *J Clim* 27:6591–6611
- Zhu X, Bye J, Fraedrich K et al (2016) Statistical structure of intrinsic climate variability under global warming. *J Clim* 29:5935–5947

Publisher's note Springer Nature remains neutral with regard to jurisdictional claims in published maps and institutional affiliations.

Affiliations

Shoupeng Zhu^{1,3} · Fei Ge^{2,3} · Yi Fan^{1,4} · Ling Zhang¹ · Frank Sielmann⁵ · Klaus Fraedrich³ · Xiefei Zhi¹

¹ Key Laboratory of Meteorological Disaster, Ministry of Education (KLME) / Collaborative Innovation Center on Forecast and Evaluation of Meteorological Disasters (CIC-FEMD), Nanjing University of Information Science & Technology, Nanjing, China

² School of Atmospheric Sciences / Plateau Atmosphere and Environment Key Laboratory of Sichuan Province/Joint Laboratory of Climate and Environment Change, Chengdu University of Information Technology, Chengdu, China

³ Max Planck Institute for Meteorology, Hamburg, Germany

⁴ Nansen-Zhu International Research Centre, Institute of Atmospheric Physics, Chinese Academy of Sciences, Beijing, China

⁵ Meteorological Institute, University of Hamburg, Hamburg, Germany